



Theme: Advancements in Amorphous Solid Dispersions to Improve Bioavailability

Preparation and Evaluation of Novel Supersaturated Solid Dispersion of Magnolol

Theme: Advancements in Amorphous Solid Dispersions to Improve Bioavailability

Jing Zhao¹ · Pan Gao¹ · Chengqiao Mu² · Jingqi Ning³ · Wenbin Deng¹ · Dongxu Ji¹ · Haowei Sun² · Xiangrong Zhang⁴ · Xinggong Yang²

Received: 9 September 2021 / Accepted: 10 March 2022 / Published online: 24 March 2022
© The Author(s), under exclusive licence to American Association of Pharmaceutical Scientists 2022

Abstract

This article aimed to design a new type of supersaturated solid dispersion (NS-SD) loaded with Magnolol (Mag) to raise the oral bioavailability in rats. In the light of the solubility parameters, phase solubility experiments, inhibition precipitation experiment, and *in vitro* release experiment, Plasdone-630 (PS-630) was selected as the optimum carrier. In addition, Mag-NS-SD was prepared by adding Monoglyceride (MG) and Lecithin High Potency (LHP) into the Mag-S-SD (Mag:PS-630 = 1:3), so as to reduce the dosage of carrier and improve the release rate. Using central composite design of response surface method, the prescription was further optimized. As the optimized condition was Mag:PS-630: MG:LHP = 1:3:0.8:0.266, the drug release rate was the fastest. Besides, after 45 min, the release rate was nearly 100%. The constructed Mag-S-SD and Mag-NS-SD were characterized by powder X-ray diffraction and infrared absorption spectrum. The XRD patterns of Mag-S-SD and Mag-NS-SD indicated that all APIs were amorphous. The IR spectra of Mag-S-SD and Mag-NS-SD demonstrated the existence of hydrogen bonding in the systems. Furthermore, *in vivo* pharmacokinetic study in rats revealed that compared with Mag and Mag-S-SD, Mag-NS-SD significantly increased the bioavailability (the relative bioavailability was 213.69% and 142.37%, separately). In this study, Mag-NS-SD was successfully prepared, which could improve the oral bioavailability and may increase the clinical application.

KEY WORDS magnolol · novel supersaturated solid dispersion · oral bioavailability · supersaturated drug delivery system (SDDS)

Jing Zhao and Pan Gao have contributed equally to this work and share first authorship.

Theme: Advancements in Amorphous Solid Dispersions to Improve Bioavailability

✉ Xiangrong Zhang
xrzhxr@126.com

✉ Xinggong Yang
yangxg321@163.com

¹ School of Traditional Chinese Medicine, Shenyang Pharmaceutical University, No.103, Wenhua Road, Shenyang 110016, China

INTRODUCTION

Oral administration is the most preferred route of drug delivery for systemic therapy, which has the characteristics of low cost, easy to carry, and good patient compliance (1). According to statistics, nearly 40% of the drug candidates have been eliminated because of their low solubility (2),

² School of Pharmacy, Shenyang Pharmaceutical University, No.103, Wenhua Road, Shenyang 110016, China

³ Wuya College of Innovation, Shenyang Pharmaceutical University, No.103, Wenhua Road, Shenyang 110016, China

⁴ Faculty of Functional Food and Wine, Shenyang Pharmaceutical University, No.103, Wenhua Road, Shenyang 110016, China

which limits the possibility of these potentially active compounds to become drugs. It is well known that solubility is a crucial factor affecting the bioavailability of drugs, especially oral drugs. As the drug must be dissolved in the aqueous intestinal contents before it can be absorbed from the gastrointestinal tract (3). For insoluble drugs, the solubility of drugs is the rate-limiting step of drug oral absorption (4).

Supersaturated drug delivery system (SDDS) is a new drug delivery system that can induce to generate a supersaturated drug solution and maintain it for a certain period of time when the drug is exposed to the drug delivery environment, thus it facilitates drug absorption and improves its bioavailability (5). Higuchi (6) was the first to find that the supersaturated state has a significant impact on drug's membrane permeability and can promote drug absorption. With the increasing research of SDDS, researchers gradually turn their attention to the research on the drug application of this system, and they found that this drug release system is very ideal for oral delivery of insoluble drugs. SDDS makes the concentration of the drug to exceed the saturation solubility in the GIT. Theoretically, high concentration has a strong driving force of drug flux through the gastrointestinal membrane and maintains the high concentration in a sufficient time period, which can enhance absorption of drugs (5). In addition, SDDS does not require much solubilizing excipients, which can effectively decrease the amount of excipients and increase the drug loading. In summary, SDDS has a huge potential in improving insoluble drugs' solubility and oral bioavailability (7).

When using SDDS as a strategy to enhance oral absorption of insoluble drugs, two essential steps of SDDS are needed: forming and stabilizing the supersaturated state of drugs. Guzman *et al.* (8) vividly described the way as "spring and parachute." The presence of a high energy form of the drug in the system can induce the generation of a thermodynamically unstable supersaturated drug solution, namely "Spring." As a result, its thermodynamic instability induces the tendency of reaching a state of equilibrium. To take full advantage of the supersaturated state of drugs produced in the GIT and promote drug absorption, precipitation inhibitors (9) can be added to interfere with the growth of crystal nucleus and slow the formation of production of precipitation (a "parachute"). The SDDS can induce supersaturation mainly in the following forms: (1) high-energy drug solid system with rapid dissolution or high apparent solubility; (2) highly concentrated drug solution system (5, 7, 10, 11). More wide applications of SDDS in pharmaceuticals are as follows.

Amorphous solid dispersion (ASD) is a typical SDDS, in which most of the active components are embedded in the solid matrix in amorphous state (11). ASDs are designed to increase drug absorption by increasing the apparent solubility or dissolution rate of the drug to produce supersaturated

solutions. The properties of dissolution strongly depend upon the physical form, crystallinity, particle size, and drug dispersibility (12). The maintenance of the supersaturated state can be achieved by using different polymers such as hydroxypropyl methylcellulose (HPMC) (13), hydroxypropyl methyl cellulose acetate succinate (HPMCAS) (14), and polyvinylpyrrolidone (PVP) (15). Within a certain proportion of drug and carriers, drug absorption can be promoted by increasing the proportion of drug and carriers and increasing supersaturation in ASDs. However, high supersaturation often leads to rapid precipitation of drugs, which is not conducive to oral absorption of drugs (8, 16). This limits its further application of S-SD in increasing the oral bioavailability of insoluble drugs.

Supersaturation self-emulsifying drug delivery system (S-SEDDS) is formed by adding precipitation inhibitors to the conventional SEDDS, which can reduce the surfactant side effects and achieve rapid absorption (10). The addition of polymers such as HPMC (17) and PVP (18) to the S-SEDDS can enable the binding of the free drug released from S-SEDDS and microemulsion to reach supersaturation in the GIT. S-SEDDS can maintain the supersaturated state, increase drug absorption *in vivo*, and increase the oral bioavailability of insoluble drugs. However, there is a large amount of lipid excipients in S-SEDDS, and the digestion of lipid excipients in the GIT after oral administration may decrease the solubility of the drug, resulting in the precipitation of the drug and reducing the absorption efficiency of the drug (19). Additionally, to resolve the question that liquid emulsion is not convenient to store and transport, the research on liquid emulsion curing is increasing gradually. Among them, adsorbing liquid emulsion on porous carriers to cure is widely used (20, 21). However, this approach also presents disadvantages as follows: different adsorption carriers have great influence on the adsorption rate of liquid preparation (22), and the addition of adsorbents leads to the increase of a unit dose (23).

Magnolol (Mag), a biphenolic compound, isolated from the bark of *Magnolia officinalis*, is widely used in traditional Chinese and Japanese medicines. Modern pharmacological research has revealed that Mag has multiple properties, including anti-inflammatory, antibacterial, and antioxidant properties (24, 25). However, the poor aqueous solubility of Mag significantly limits its oral bioavailability and therapeutic activity. In this study, the novel supersaturated solid dispersion of Mag (Mag-NS-SD) was prepared by adding self-emulsifying excipients to the conventional ASDs which can combine the advantage and overcome the drawbacks of ASDs and S-SEDDS. Mag-NS-SD retains the advantages of traditional ASDs and S-SEDDS, such as simple preparation process, convenient storage and transportation, and improving the solubility, dissolution rate, and oral bioavailability of poorly soluble drugs. In addition, Mag-NS-SD can

effectively reduce the amount of carriers and increase drug loading. Also, Mag-NS-SD can reduce the amount of lipid excipients and surfactants, improve the stability in GIT, and reduce toxicity.

MATERIALS AND METHODS

Materials

Mag and Osthol (OST) were provided by Nantong Feiyu Biotechnology Co., Ltd. (Jiangsu, China). Monoglyceride (MG) and Lecithin High Potency (LHP) were obtained from Gattefossé Co. (Lyon, France). Polyvinyl caprolactam-polyvinyl acetate-polyethylene glycol copolymer (Soluplus) was kindly donated by BASF (Ludwigshafen, Germany). Polyvinylpyrrolidone-K30 (PVP K30) and vinyl pyrrolidone and vinyl acetate copolymer (PVP VA64) were purchased from Anhui Shanhe Medicinal Accessories Co., Ltd. (Anhui, China). PlasdoneS-630 (PS-630) was purchased from Ashland Co., Ltd. Heparin sodium (> 150 IU/mg) was received from the Dalian Meilun Biological Technology Co., Ltd. (Liaoning, China). All other chemicals used in the experiments were analytical reagent grade and were obtained from local sources.

Preparation of Mag-SDDS

Preparation of Mag-S-SD

In this study, we employed solvent volatilization method to prepare Mag-S-SD. A mixture consisting of Mag and carriers were dissolved in methanol through continuous stirring at ambient temperature. A clear solution was obtained. The resulting solution was evaporated, by a rota-evaporator under the condition of 45 °C, 70 r·min⁻¹. The dried samples were crushed and filtered through 80-mesh screen.

In this study, PS-630, PVP VA64, PVP K30, and Soluplus, water-soluble carrier materials which have been successfully produced in industrial scale and whose safety have been fully studied, are selected to prepare. They can improve the wettability of drugs, effectively improve the drug solubility, and accelerate the rate of drug dissolution, thus they improve the bioavailability of drugs. PS-630, PVP VA64, and PVP K30 are all povidone carrier materials, which have the advantages of inhibiting drug crystallization and stabilizing drug's amorphous or molecular state in carrier materials (26, 27). Soluplus is a new type of surfactant and an amphiphilic triblock copolymer with low viscosity and good fluidity. Soluplus can not only reduce the surface tension but also increase the miscibility of drugs and excipients, improve the wettability of solid dispersion, and effectively reduce the recrystallization of drugs (28, 29).

Preparation of Mag-NS-SD

A mixture consisting of Mag and carriers were dissolved in isopropanol through continuous stirring at 70 °C. A clear solution was obtained. The resulting solution was evaporated, by a rota-evaporator under the condition of 70 °C, 70 r·min⁻¹. The samples were stored at -20 °C for 12 h. The dried samples were crushed and filtered through 80-mesh screen.

Single Factor Screening Experiments

Solubility Parameter

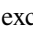
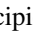
Solubility parameter is widely used in many different fields, among which pharmaceuticals is the main discipline in which solubility parameter is applied to formulation design. Solubility parameter is widely used for predicting compatibility between two materials (30–32). The compatibility between drugs and carriers is a key indicator for screening the carriers of solid dispersion. Compatibility reflects the mixability between the drug and the carriers. From the molecular level, compatibility reflects the strength of molecular interaction on the premise of no chemical reaction between the drug and the carrier (33). In general, the higher the compatibility between the drug and the carriers, the stronger the interaction between them. Therefore, it is easier to prepare solid dispersions, making for better drug release and more stable storage (34, 35). Solubility parameter (δ) was first applied to screen the carrier of solid dispersions in 1999. The compatibility can be studied by difference of solubility parameters between drugs and carriers ($\Delta\delta$). When $\Delta\delta < 7.0 \text{ MPa}^{0.5}$, the compatibility of drug and carriers was good. When $\Delta\delta > 10.0 \text{ MPa}^{0.5}$, the compatibility was poor. The solubility parameter was calculated using the Fedors group contribution method. The solubility parameter can be rapidly calculated by the chemical structure formula of organic compounds (36) as follows.

$$\Delta E = \sum \Delta e_i \quad (1)$$

$$V = \sum \Delta v_i \quad (2)$$

$$\delta = \left(\frac{\sum \Delta e_i}{\sum \Delta v_i} \right)^{0.5} \quad (3)$$

where δ , Δe_i , Δv_i , ΔE , and V are the solubility parameter, the evaporative energy of the group, the molar volume of the group, the evaporative energy, and the molar volume.

The chemical structural formula (Fig. 1) of Mag was separated as $2 \times$ , $2 \times$ -OH, $2 \times$ , $2 \times$ =CH- and $2 \times$ =CH₂. The solubility parameter of Mag was calculated by Fedors group contribution method, and the results are shown in Table I.

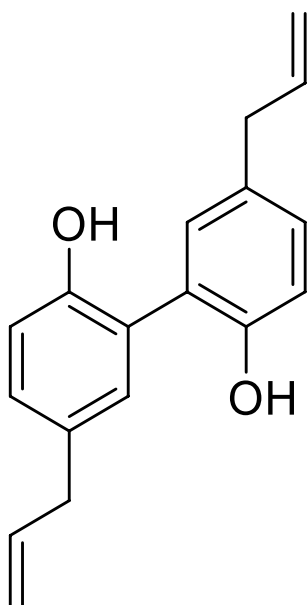


Fig. 1 The constitutional formula of Mag

And a summary of the solubility parameters of carriers and Mag is shown in Table II (37–39).

Phase Solubility Experiments

The mother liquor was prepared by weighing 1800 mg of carrier and then dissolved in 60 mL water. The above mother

liquor was diluted in a standard series with water, and the concentrations were 0.5, 1, 2, 4, and 6 mg·mL⁻¹. After that, 7 mL was taken from this solution and put it in the 10 mL bottle. After adding excess Mag powder, the sample was placed for 72 h at 37 °C in a shaker with 100 r·min⁻¹ shaking. After filtered with a 0.45 μm filter membrane, the absorbance of solution was determined by UV–vis spectrophotometer, and the concentration of Mag was calculated by external standard method after the filtrate was diluted with methanol (40, 41). The polymer concentration (mg·mL⁻¹) was taken as the ordinate and the Mag solubility (μg·mL⁻¹) was considered the abscissa to obtain a linear regression equation. Set the UV wavelength to 291 nm. The linearity of Mag was good in the range of 12–28 μg·mL⁻¹, and the correlation coefficient was greater than 0.999 (a standard curve: $A = 0.0274C - 0.0029$). The relative standard deviation of intra-day accuracy was less than 2%.

Inhibit Precipitation Experiment

Supersaturated solid dispersions increased the solubility and dissolution of insoluble drugs by dissolving the drugs in the medium to form supersaturated solution. It should also be considered that “spring” and “parachute” were necessary to achieve effective solubilization (42). In this study, supersaturation was investigated using the solvent-shift method (43, 44). 150 mg Mag was dissolved in 3 mL dimethyl sulfoxide (DMSO) to be 50 mg·mL⁻¹ of final concentration. Mag solution (0.4 mL) was added to a 50 mL

Table I The Calculation of Solubility Parameter for Mag

Group	Qty.	Δe_i	Δe_i	Δv_i
		cal·mol ^{0.5}	J·mol ^{0.5}	cm ³ ·mol ^{0.5}
	2	7630	63876.10	33.40
—OH	2	5220	43700.29	13.00
	2	1180	9878.61	16.10
=CH—	2	1030	8622.85	28.50
=CH ₂	2	1030	8622.85	13.50

1 cal = 4.1858518 J

Table II The Results of Solubility Parameters of Drug and Carriers

Drug/carrier	δ (MPa ^{0.5})	$\Delta\delta$ (MPa ^{0.5})	Ref
Magnolol	25.38	-	Calculated
Mannitol	38.2	12.82	(32)
Lactose	36.3	10.92	(33)
Citric acid	33.8	8.42	(34)
Urea	38.5	13.12	(35)
PS-630	22.94	2.44	(36)
PVP K30	25.12	0.26	Calculated
PVP VA64	24.44	0.94	Calculated
Soluplus	24.18	1.2	Calculated

carrier solution (2 mg·mL⁻¹). When the temperature was kept at 37 ± 0.5 °C, the rotational speed was maintained for 100 r·min⁻¹. Samples were sampled at 0, 10, 30, 45, 60, 90, 120, 180, and 240 min and 5 mL samples were taken at each time point (without supplement). The samples were filtered through a 0.45 µm filter. The concentration of Mag was assayed by UV–vis spectrophotometer after appropriate dilution with methanol. The UV wavelength was set at 291 nm. The pure water solution without carrier was used as the control.

In Vitro Release Experiment

The samples were Mag-S-SD (an amount equal to 40 mg Mag, Mag: carrier = 1:5, w/w) and the same dose of Mag. According to the second method of General Rule 0931, Part IV of Chinese Pharmacopoeia 2015 edition, release medium was 900 mL 0.05% SDS, temperature was kept at 37 ± 0.5 °C, and the rotational speed was 100 r·min⁻¹. 5 mL samples were respectively taken at 5, 10, 15, 30, 45, 60, 90, 120, and 180 min. Then the solution was filtered by 0.45 µm microporous membrane, and the primary filtrate was discarded. The subsequent filtrate was taken for detection, and 5 mL blank medium was immediately added. UV–vis spectrophotometer was used to determine the dissolution rates at different time points.

Optimization of Mag-S-SD

Supersaturation Degrees Tests

The main purpose of this experiment was to measure the supersaturation degree at different proportions of Mag/carrier. Supersaturation degrees (*S*) in solution can be defined as the ratio of instantaneous drug concentration to equilibrium drug solubility in the corresponding polymer solution. In the experiment, the instantaneous drug concentration was the drug concentration measured after Mag-S-SD was

uniformly dispersed in water, that was, C_0 . The equilibrium solubility was the solubility of the drug when the equilibrium was reached when excessive Mag powder was added to the excipient solution of the formulation, that as, C_{eq} . Therefore, the supersaturation of supersaturated system can be calculated according to Eq. 4. The calculation results of *S* are shown in Tab III.

$$S = \frac{C_0}{C_{eq}} \quad (4)$$

In Vitro Release Experiment

The samples were Mag-PS-630-SD (an amount equal to 40 mg Mag, Mag:PS-630 = 1:2–1:6, w/w) and the same dose of Mag raw material. The specific experimental process was the same as mentioned above.

Characterization of Mag-S-SD

Particle Size

The micellar particle sizes of Mag-PS-630-SD in different ration of Mag and PS-630 dispersed evenly in water were determined by dynamic light scattering method on Zeta sizer (Nano-ZS, Malvern instruments, UK) after equilibrating at 25 °C for 240 s. Each preparation was filtered by 0.45 µm stream needle filtration membrane before particle size determination. The measurement of each sample was repeated in triplicate.

Powder X-Ray Diffraction

Powder X-ray diffraction (PXRD) is an important detection method for crystal characterization of compounds. Different crystal spatial morphologies can be effectively distinguished by specific diffraction line distribution position (2θ) and intensity (I/I_0). Samples were exposed to Cu radiation under 40 mA and 40 kV. The scanning angle (2θ) ranged from 2° to 45° at 0.02°/s.

Table III Instantaneous Drug Concentration (C_0), Drug Equilibrium Solubility in PS-630 Solutions (C_{eq}), and Supersaturation Degrees (*S*) at Different Ratios of Mag and PS-630 ($n = 3$)

Mag/PS-630 ratios	C_0 (µg·mL ⁻¹)	C_{eq} (µg·mL ⁻¹)	<i>S</i>
1:2	79.85	24.06	3.32
1:3	93.57	36.83	2.54
1:4	99.21	52.29	1.90
1:5	108.89	72.06	1.51
1:6	111.31	99.35	1.12

Infrared Absorption Spectrum

Infrared (IR) absorption spectroscopy can reflect the interaction between drugs and carriers. If there is some interaction or reaction between the drug and the carrier, the shift or strength of the absorption peak will change. Mag, PS-630, physical mixture (PM), and Mag-PS-630-SD (SD) were ground and mixed with KBr powder, respectively, and the samples were analyzed in the range of 400–4000 cm^{-1} .

Optimization of Mag-NS-SD

The pre-experiment showed that Mag-NS-SD by adding MG and LHP, which had good solubility to Mag, can significantly improve the dissolution rate and cumulative dissolution of Mag. Moreover, with the addition of lipid excipients, the Mag-NS-SD had the advantages of S-SD and S-SEDDS at the same time. In this study, a central composite design (CCD) was used to optimize the Mag-NS-SD (45). In this study, CCD which is two-factor, five-level face-centered was used for optimizing the prescription of Mag-NS-SD. The ratio of oil phase to emulsifier (X_1) and the ratio of carrier to oil phase (X_2) were taken as critical factors, and the cumulative release (%) of each Mag-NS-SD at 15 min was taken as the response value. The horizontal code values and practical values of indexes are showed in Table IV. CCD was determined in random order and designed by Design-Expert 8.0 software (MN, USA) (46). And the fitted polynomial equation was described by the 3D response surface diagram.

In Vitro Release Experiment in Different Release Mediums

The samples were Mag, Mag-S-SD, and Mag-NS-SD (an amount equal to 40 mg Mag). The release mediums were hydrochloric acid solution (HCl, pH 1.2), phosphate-buffered saline solution (PBS, pH 4.5 and 6.8), and water. To achieve a sink condition, 0.05% SDS was added, respectively. The specific experimental process was the same as mentioned above.

Table IV Levels of Independent Variable in the Central Composite Design

Factor	Level				
	-1.732	-1	0	+1	+1.732
X_1	0.172	1.00	3.00	5.00	5.83
X_2	0.57	1.5	3.75	6	6.93

Characterization of Mag-NS-SD

Particle Size

The particle size of Mag-S-SD (Mag:PS-630 = 1:3) and Mag-NS-SD was identified by using a Zeta sizer (Nano-ZS, Malvern instruments, UK) at 25 °C. The measurement for each sample was repeated in triplicate.

Supersaturation Degrees Tests

The samples were Mag-S-SD (Mag:PS-630 = 1:3) and Mag-NS-SD. The next steps were same as mentioned above.

Powder X-Ray Diffraction

The samples were Mag, Mag-NS-PM, and Mag-NS-SD. The next steps were same as mentioned above.

Infrared Absorption Spectrum

The samples were Mag, Mag-NS-PM, and Mag-NS-SD. The next steps were same as mentioned above.

In Vivo Pharmacokinetic Study

Animal Experiment

Male Sprague Dawley rats (weight 200 ± 20 g, healthy, $n = 15$) were divided into two groups at random (provided by Animal Center of Shenyang Pharmaceutical University). After fasting for 12 h, the administration scheme and blood sample collection experiment were carried out. The Mag, Mag-S-SD, and Mag-NS-SD suspended in 0.5% sodium carboxymethylcellulose (CMC-Na) solution were administered by gavage at $80 \text{ mg}\cdot\text{kg}^{-1}$, and after 4 h, free drinking water was supplied. 500 μL blood was respectively taken from orbital venous plexus at 0.167, 0.5, 1, 2, 4, 6, 8, 12, and 24 h after administration. The centrifuge speed was set to $5000 \text{ r}\cdot\text{min}^{-1}$ and the temperature was set to 4 °C. The plasma separated by a pipette gun was frozen in the refrigerator at -20 °C.

Analysis of Mag in Plasma

Plasma samples of 200 μL were added with the 25 μL of internal standard solution (Osthol, $30 \mu\text{g}\cdot\text{mL}^{-1}$). After vortex 2 min, 1000 μL of acetonitrile was added. Then the samples were vortex-mixed for 2 min. After centrifugation at $8000 \text{ r}\cdot\text{min}^{-1}$ for 10 min, the organic layer was collected and evaporated to dryness at 40 °C under a mild nitrogen flow. The concentrate was re-dissolved in 100 μL mobile phase, vortex for 2 min. After centrifugation at $10,000 \text{ r}\cdot\text{min}^{-1}$ for 10 min,

20 μL supernatant was injected into an HPLC system, which equipped with a UV detector set at 291 nm. The analytical column was Phenomenex C18 column (150 mm \times 4.60 mm, 5 μm). The flow rate was kept at 1 mL $\cdot\text{min}^{-1}$ and the column temperature was set at 35 $^{\circ}\text{C}$. The mobile phase was made up of 0.1% phosphoric acid and acetonitrile with the 60/40 (v/v) ratio. The linear range of this method was 0.05–6.4 $\mu\text{g}\cdot\text{mL}^{-1}$, and an R^2 (correlation coefficient) was 0.9939. The precision and accuracy results of three different concentrations in the calibration range exhibited fine precision and accuracy (RSD < 15%). The recoveries of three different control samples ranged from 85 to 115%, and the coefficient of variation was no more than 15%.

Pharmacokinetic Analysis

The results were expressed in the form of mean \pm SD. Besides, one-way analysis of variance (ANOVA) was used to compare the statistical significance of data from different formulations.

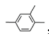
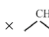
Ethical Approval

All animal research work in this study was approved by the Life Science Research Center and Ethical Committee. All animal study protocols (license NO. SYPU-IACUC-C-2020–21-004) had been approved and signed by the Institutional Animal Care and Use Committee (IACUC) at Shenyang Pharmaceutical University before the animal experiment. All efforts were made to ensure the welfare of animals and minimize the pain of animals. At the end of the experiment, the animals were euthanized.

RESULTS AND DISCUSSION

Single Factor Screening Experiments

Solubility Parameter

The chemical structural formula (Fig. 1) of Mag was separated as $2 \times$ , $2 \times$ $-\text{OH}$, $2 \times$ , $2 \times$ $=\text{CH}-$ and $2 \times$ $=\text{CH}_2$. The solubility parameter of Mag was calculated by Fedors group contribution method, and the results are shown in Table I. According to Eq. 1, we can obtain that $\Delta E = \sum \Delta e_i = 134,700.71$, according to Eq. 2, we can obtain that $V = \sum v_i = 209.00$, and according to Eq. 3, we can obtain that $\delta = (\sum \Delta e_i / \sum v_i)^{0.5} = 25.38 \text{ MPa}^{0.5}$. Based on the literature search and Fedors group contribution method, a summary of the solubility parameters of carriers and Mag is shown in Table II. The results showed that the $\Delta\delta$ of PS-630, PVP K30, PVP VA64, and Soluplus with Mag were all less than 7.0 $\text{MPa}^{0.5}$, indicating that these carriers were

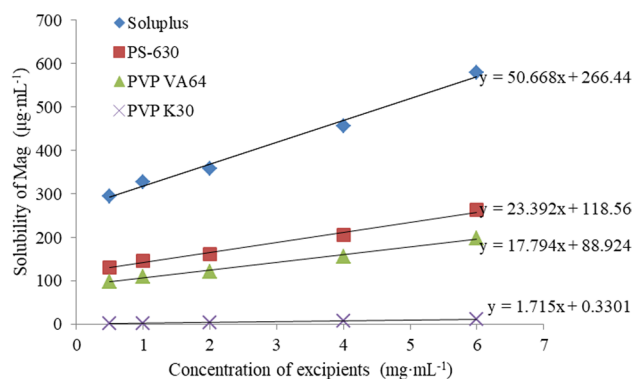


Fig. 2 Phase solubility of Mag in aqueous solution of PS-630, PVP K30, PVP VA64, and Soluplus at 37 $^{\circ}\text{C}$ ($n=3$)

easily miscible with Mag in theory. Therefore, these carriers were used as potential carriers for the preparation of Mag-S-SD.

Phase Solubility Experiments

It can be seen from Fig. 2 that there was a linear relationship between the concentration of Mag and carriers. When the concentration of each carrier was the same, the steeper slope of the regression line was and the larger concentration of Mag was, indicating that the stronger the ability to solubilize. Therefore, it can be concluded that the steeper slope of the regression line was, and the stronger capacity of the carriers was. According to Fig. 2, the order of solubilization ability of carriers was Soluplus > PS-630 > PVP VA64 > PVP K30. The determination of the solubility of Mag in different concentrations of carrier solution can reflect the solubility of Mag in the carriers. In this study, the solubilization ability of different carriers to Mag was investigated by phase solubility experiment, and the ability to maintain supersaturated state and drug release were further investigated by supersaturation tests and *in vitro* release tests.

Inhibit Precipitation Experiment

From Fig. 3, it can be seen that there was a noticeable trend of Mag in pure aqueous solution without carrier. After Mag concentrate was added to pure water, the drug precipitated rapidly and the amount precipitated was reached 80% within 10 min. The different carriers had remarkably different supersaturated maintenance capacities. When Mag concentrate was added to the carrier solution, the difference of Mag concentration with time was significant. Of those, Soluplus had the strongest supersaturated maintenance capacities of Mag. PS-630 was the next and it was observed that there was some precipitation in PS-630 solution, but it can effectively maintain the supersaturation of Mag throughout the

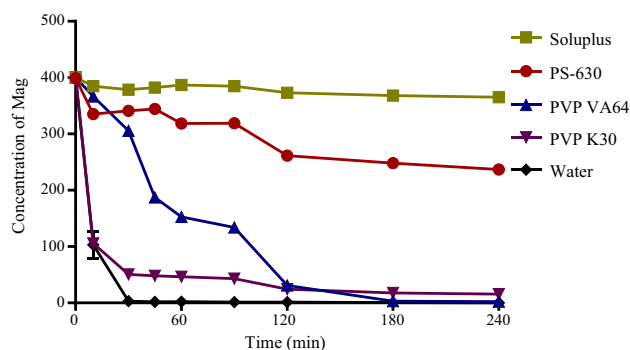


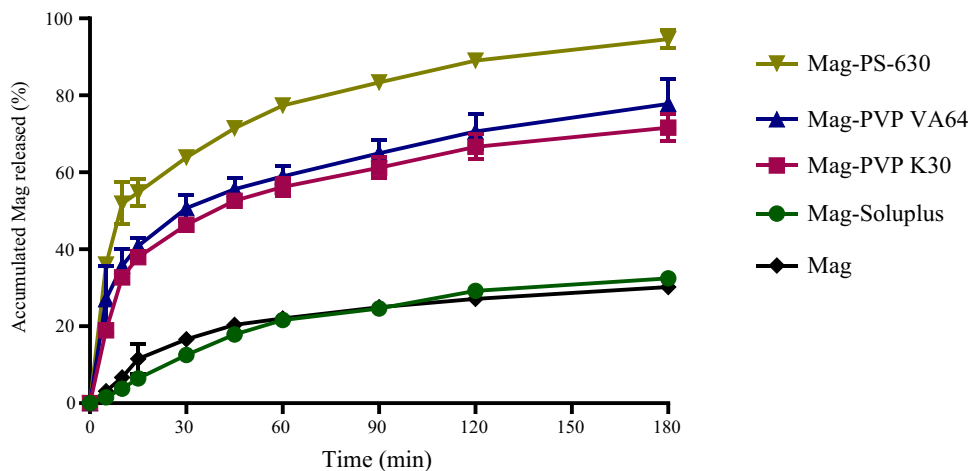
Fig. 3 Effect of different excipients on the maintenance of Mag supersaturation ($n = 3$)

test. And the ability of PVP VA64 and PVP K30 to maintain supersaturation was poor. According to Fig. 3, the order of maintaining supersaturation ability of carriers was Soluplus > PS-630 > PVP VA64 > PVP K30. The order was the same as the order of solubilization ability of carriers in Fig. 2. Inhibit precipitation experiments reflected the abilities of the carriers to maintain drug supersaturation. Because high concentration had a greater driving force for drug flux through the gastrointestinal membrane, the stronger the ability to maintain supersaturated state in a sufficient period of time, the more conducive to drug dissolution, which can achieve the purpose of enhancing absorption. Phase solubility experiments and inhibit precipitation experiments showed that Soluplus can effectively maintain the metastable state of Mag's supersaturated solution for a long time and improve the drug concentration of Mag, followed by PS-630 and PVP VA64, and PVP K30 is the worst.

In Vitro Release Experiment

According to Fig. 4, the release behaviors of Mag-S-SD prepared by different carriers were different in 0.05% SDS

Fig. 4 The effect of different excipients on dissolution profile of Mag in aqueous water containing 0.05% SDS ($n = 6$)



solution. The result displayed that Mag release rate was slow and the cumulative drug release was only $(30.20 \pm 0.41)\%$ within 3 h. Both Mag-S-SD showed enhanced dissolution rate as compared to pure drug. Among them, the dissolution rate and cumulative release rate of Mag-PS-630-SD were better than those of other SD, and the cumulative drug release was $(94.64 \pm 2.28)\%$ within 3 h. In contrast, the dissolution rate and cumulative release of Mag-PVP VA64-SD and Mag-PVP K30-SD were poor. The above results were similar to the experimental results of phase solubility experiments, but the result of Mag-Soluplus-SD was quite different from that of phase solubility experiments. In the phase solubility experiments, Soluplus had the better solubilization ability to Mag than the other carriers, but in the *in vitro* dissolution experiment, it was found that the release of Mag-Soluplus-SD was very poor, even similar to that of the raw material drug. The solid dispersion prepared with Soluplus as carrier is difficult to release. The cause of this may be that Soluplus was an amphiphilic triblock copolymer with low critical micelle concentration ($CMC = 7.6 \text{ mg/mL}$) and was easy to self-assemble to form polymer micelles in water (47, 48). In combination with the solubility parameters, Soluplus is more compatible with Mag than PS-630, and it is the strong interaction between them that led to the poor release of Mag-Soluplus-SD (28, 29).

Pooled analysis of solubility parameters, phase solubility experiments, inhibit precipitation experiments, and *in vitro* release experiments showed that Soluplus had a good solubilization effect on Mag and the ability to maintain supersaturated state effectively. However, because of the strong interaction between the drug and the hydrophobic polymer micelle core in Mag-Soluplus-SD, it was difficult for Mag to release *in vitro*. In contrast, although the ability of PS-630 to maintain the supersaturated state of Mag was slightly poor, it was still significantly better than PVP VA64 and PVP K30. In addition, Mag-PS-630-SD had a good release *in vitro*. To

sum up, through the single factor experiments, the optimal carrier was selected as PS-630.

Optimization of Mag-S-SD

Supersaturation Degrees Tests

Through the single factor experiments, it was determined that the optimal carrier of Mag-S-SD was PS-630. The main purpose of this experiment was to measure *S* at different proportions of Mag/PS-630. From Table II, it was found that *S* of Mag-PS-630-SD increased with the increase of Mag/PS-630 mass ratio. When the ratio of Mag/PS-630 was from 1:2 to 1:6, *S* was 3.32, 2.54, 1.90, 1.51, and 1.12, respectively. The dissolution of Mag-S-SD with different supersaturation needs to be further investigated according to the dissolution experiment.

In Vitro Release Experiment

From Fig. 5, it can be seen that the cumulative drug release of Mag-PS-630-SD tended to increase with increase in the proportion of carriers, and the dissolution profiles were significantly superior to that of Mag. When Mag:PS-630 = 1:6, dissolution profiles were the best, and the drug was almost completely released at 1 h reaching to (97.97 ± 0.11)%. The dissolution profiles decreased when the ratio of Mag and PS-630 was 1:5 or 1:4, and the cumulative release was less than 80% at 1 h. When the ratio of Mag and PS-630 was 1:3 or 1:2, the *in vitro* dissolution of Mag-S-SD was even worse, and the cumulative release was less than 60% at 1 h.

Comprehensive supersaturation degrees tests and *in vitro* release experiment results found that the drug release of Mag-S-SD with higher supersaturation was slower. This may

be because the supersaturation was higher, and the supersaturated solution was formed in the water media but cannot be effectively maintained. This supersaturated state led to the precipitation of the drug and slowed the drug release.

In this study, Mag:PS-630 = 1:6 had the best dissolution profile, but the carrier dosage was large, which restricted the drug ability. Therefore, to reduce the amount of carrier, the formulation of Mag:PS-630 = 1:2 should be selected for further optimization, but it was found that the Mag-PS-630-SD (1:2, w/w) powder had poor fluidity and was easy to agglomerate. Therefore, the formulation of Mag:PS-630 = 1:3 was selected for further optimization, to reduce the amount of carrier, effectively maintain the metastable state of the supersaturated system, improve the dissolution rate and cumulative dissolution of the drug, and lay the groundwork for improving the oral bioavailability of Mag.

Characterization of Mag-PS-630-SD

Particle Size

As an organic polymer compound, PS-630 is a linear copolymer obtained by the reaction of N-vinyl pyrrolidone and ethyl acetate at 3:2. There are both hydrophilic N-vinyl pyrrolidone and hydrophobic ethyl acetate in the structure of PS-630, which makes it amphiphilic. Therefore, when PS-630 is dispersed evenly into aqueous media, it is going to form nanoparticles. According to Fig. 6, there was a tendency towards the particle size of Mag-PS-630 nanoparticles with the increase of the ratio of Mag and PS-630 and the increase of drug loading. The reason was that Mag was solubilized in the core formed by PS-630, and with the increase of drug loading, the amount of drugs solubilized in the core will also increase, so the nanoparticle's size

Fig. 5 The effect of the ratio of Mag and PS-630 on dissolution profile of Mag in aqueous water containing 0.05% SDS (*n* = 6)

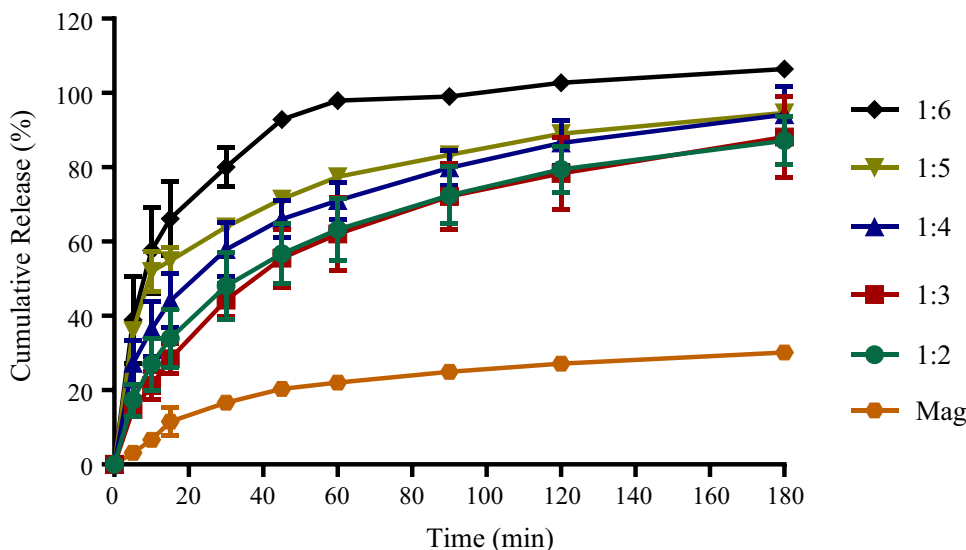


Fig. 6 The particle size (A) and polydispersity index (B) of the Mag-PS-630-SDs with different ratios of Mag and PS-630 ($n = 3$)

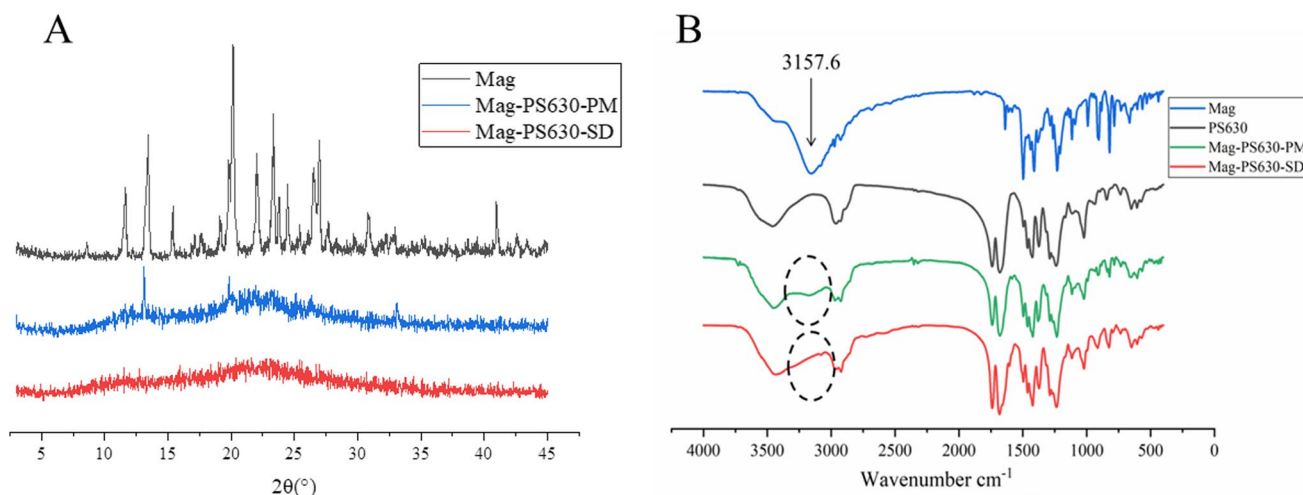
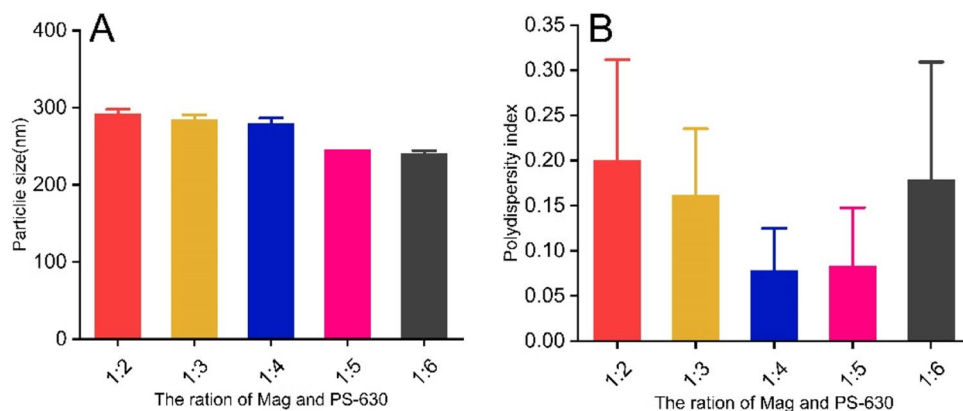


Fig. 7 PXRD diagrams (A) and IR spectra (B) of Mag, the physical mixture of Mag and PS-630 (Mag-PS-630-PM), and the Mag-PS-630 solid dispersion (Mag-PS-630-SD)

became larger. The results were consistent with the results of supersaturation (Table III). The higher the ratio of Mag and PS-630, the more drugs solubilized in the core, the higher the supersaturated state, and the larger the particle size of the nanoparticles.

Powder X-Ray Diffraction

In Fig. 7A, there were many diffraction peaks in the PXRD pattern of Mag, indicating that the Mag raw material powder mainly existed in the crystalline state. In the PM, the diffraction peak decreased obviously due to the decrease of the relative mass of Mag. In the diffraction pattern of Mag-PS-630-SD, the diffraction peak of Mag basically disappeared, indicating that most of Mag in Mag-PS-630-SD changed from crystalline to molecular or amorphous.

Infrared Absorption Spectrum

According to Fig. 1, there were phenolic hydroxyl groups in Mag. It can be seen from Fig. 7B that the absorption peak near 3157 cm^{-1} was the characteristic absorption peak of Mag. The physical mixture spectrum (Mag-PS-630-PM) of Mag and PS-630 was similar to the combination of their IR spectra, and a small characteristic frequency of -OH can still be seen at 3157.6 cm^{-1} . In the IR spectra of Mag-PS-630-SD, the -OH characteristic peak at 3157.6 cm^{-1} completely disappeared. The above results indicated that there may be hydrogen bonding between Mag and PS-630 in Mag-PS-630-SD. Hydrogen bonding interaction was considered to be an important reason why PS-630 can solubilize insoluble drugs, effectively maintain drug supersaturation, and inhibit recrystallization (49).

Table V Response of Central Composite Design

NO	Levels of independent factors		Response <i>Y</i> (%)
	X_1	X_2	
1	5.00	6.00	57.63
2	5.00	1.50	2.16
3	3.00	3.57	64.25
4	3.00	0.57	36.23
5	1.00	1.50	36.25
6	3.00	3.75	57.36
7	1.00	6.00	51.41
8	3.00	6.93	52.68
9	0.17	3.75	27.44
10	5.83	3.75	62.01
11	3.00	3.75	65.23
12	3.00	3.75	59.35
13	3.00	3.75	62.65

Optimization of Mag-NS-SD

On the basis of the preliminary experimental results, the ratio of oil to emulsifier (X_1) and the ratio of carrier and oil (X_2) played decisive roles in the cumulative release at 15 min (Y), and as such, they were taken as the major investigating factors. Table V demonstrates the independent variables of the experimental runs and their responses. Analysis of these responses by Design-Expert illustrated that for each response Y , the quadratic model was the best regression model. The mathematical model was described as follows:

$$Y = -1.07 + 15.68X_1 + 14.93X_2 + 0.02X_1X_2 - 1.99X_1^2 - 1.60X_2^2 (R^2 = 0.8756, P = 0.0045)$$

The ANOVA Y is described in Table VI. As can be seen from the table, the second-order model was significant ($*P < 0.008$), but the lack of fitting terms was not significant. The coefficient of determination (R^2) of the model Y_1 was 0.8756. The above results suggested that the error of experimental data is small. The determined values showed no difference with the predicted values, and the model fully expressed the relation among the parameters (50).

The three-dimensional (3D) response surface and contour plot for Y are described in Fig. 8. From Fig. 8A and B, it can be seen that X_1 , X_2 , and their interaction produced a significant effect on Y . The fitting results illustrated that the optimized Mag-NS-SD with high cumulative release at 15 min was acquired with the X_1 as 3 and the X_2 as 3.75, respectively. In order to verify the accuracy of the model, three parallel experiments were conducted in line with the predicted optimal formulation (Mag:PS-630: MG: LHP = 1:3:0.8:0.266). The results of the validation are

Table VI The ANOVA Results of Y

Source	Sum of squares	<i>df</i>	<i>F</i> value	<i>P</i> value	
Model	1620.39	5	9.85	0.0045	*
$A-X_1$	465.42	1	14.15	0.0071	*
$B-X_2$	363.07	1	11.04	0.127	
AB	0.024	1	7.305E-004	0.9792	
A^2	440.04	1	13.38	0.0081	*
B^2	455.11	1	13.84	0.0075	*
Residual	230.22	7			
Lack of fit	186.02	3	5.61	0.0645	Not significant
Pure error	44.20	4			
Cor total	1850.61	12			

**Significant differences ($P < 0.0001$); *differences ($P < 0.05$)

shown in Table VII. The experimental values in the optimal range were very close to the predicted values, which figured that the optimized formulation was reliable.

In Vitro Release Experiment in Different Release Mediums

According to Fig. 9, the dissolution profile of Mag was poor in every medium, and the cumulative release was almost unchanged after 1 h, all below 40%. Mag-S-SD can increase the dissolution rate and cumulative release of Mag to some extent, but still cannot achieve rapidly and completely release. Mag-NS-SD, by adding MG and LHP to Mag-S-SD, can achieve the rapidly release in different mediums. And almost 100% release was achieved after 45 min. Therefore, compared with Mag and Mag-S-SD, Mag-NS-SD can effectively improve the solubility of drugs in the whole GIT. This is due to the addition of self-emulsifying excipients (oil phase MG and amphiphilic LHP) with good solubility of Mag. The oil phase and Mag were solubilized in the core of the nanoparticles and LHP and PS-630 formed a composite surfactant which adsorbed on the oil–water interface and reduced the surface tension. This made Mag-NS-SD released faster and more completely than Mag-S-SD (51–53).

Characterization of Mag-NS-SD

Particle Size

Figure 10A is a schematic diagram of the structure of Mag-S-SD. When the concentration of amphiphilic substance PS-630 exceeded a certain concentration, the molecule formed a spherical structure with the non-polar group as the core and the polar group as the outer layer. The insoluble drug was solubilized in the non-polar core. The studies (54, 55) revealed that the micelle can

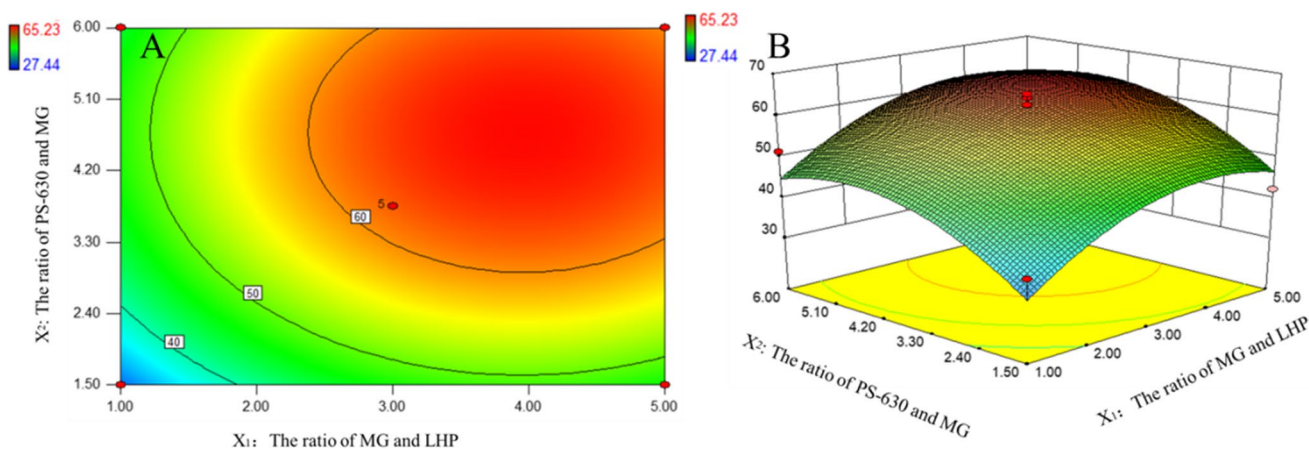


Fig. 8 Contour plot (A) and response surface (B) for cumulative release at 15 min (Y) of two factors

Table VII Predicted and Observed Values of Optimized Formulation

Response	Predicted value	Actual value	Bias (%)
Y (%)	61.77	60.98	1.27

Bias (%) = (actual value – predicted value) / predicted value × 100

significantly improve the solubilization capacity and stability of insoluble drugs after solubilizing the oil phase, which was called swollen micelle. Therefore, when the oil phase MG and amphiphilic LHP were added into the

system, according to the swollen micelle theory, the oil was correspondingly solubilized in the core of the nanoparticles, improving the solubilization capacity of insoluble drugs, and the particle size became larger. It was speculated that LHP and PS-630 should form a composite surfactant, which can be adsorbed on the oil–water interface to reduce the surface tension and make the structure more stable (43) (as shown in Fig. 10B). And the particle size results showed that the particle size of (Fig. 11) Mag-NS-SD was larger than that of Mag-S-SD, which verified the above conjecture.

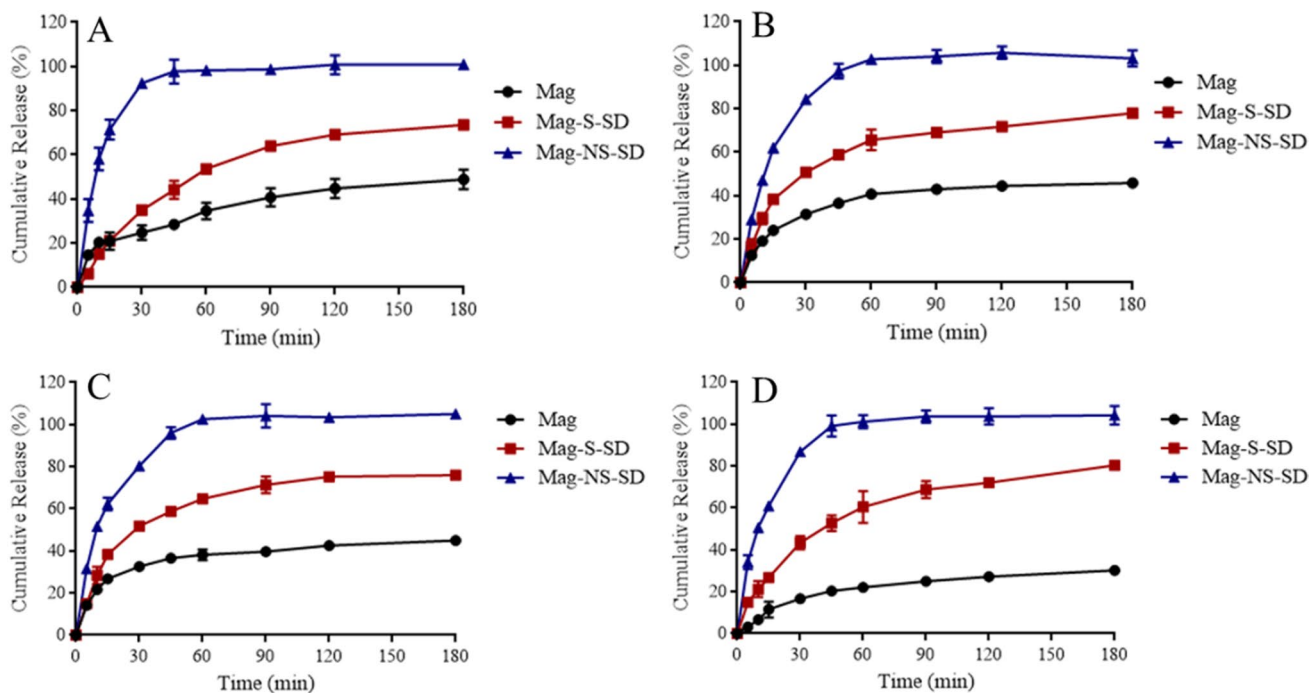


Fig. 9 The effect of different release mediums on dissolution profile of Mag, Mag-S-SD, and Mag-NS-SD (n=6). The mediums included pH 1.2 HCl (A), pH 4.5 PBS (B), pH 6.8 PBS (C), and water (D)

Fig. 10 Schematic diagrams of Mag-S-SD (A) and Mag-NS-SD (B)

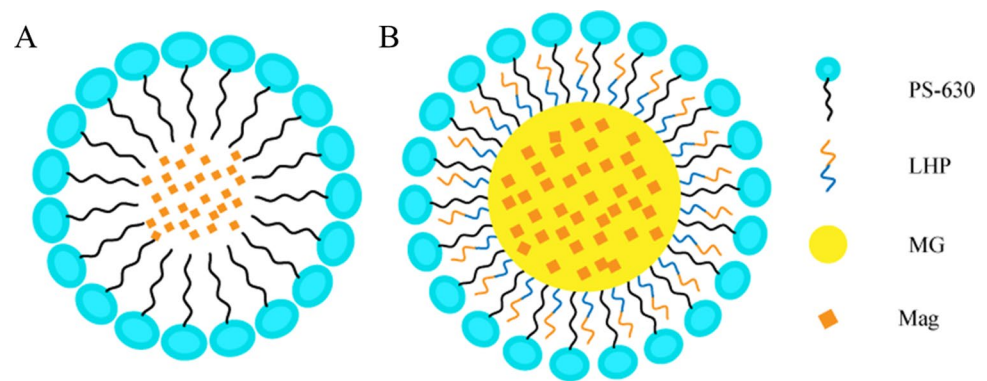


Fig. 11 The particle size (A) and polydispersity index (B) of the Mag-S-SD and Mag-NS-SD ($n=3$)

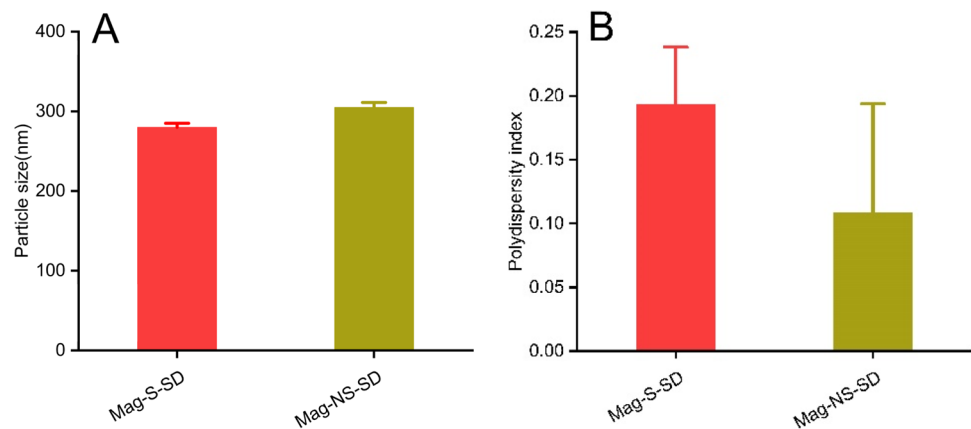


Table VIII Instantaneous Drug Concentration (C_0), Drug Equilibrium Solubility, and Supersaturation Degrees (S) at Mag-S-SD and Mag-NS-SD ($n=3$)

	C_0 ($\mu\text{g}\cdot\text{mL}^{-1}$)	C_{eq} ($\mu\text{g}\cdot\text{mL}^{-1}$)	S
Mag-S-SD	93.57	36.83	2.54
Mag-NS-SD	480.38	105.13	4.57

Supersaturation Degrees Tests

According to Table VIII, when MG and LHP with good solubility to Mag were added into Mag-NS-SD, the equilibrium solubility (C_0) and instantaneous drug concentration (C_{eq}) increased significantly, indicating that the system had stronger solubilization capacity to Mag. In addition, the supersaturation degree of Mag-NS-SD was also significantly higher than that of Mag-S-SD, and the increase of supersaturation degree can effectively promote the release of the drug, which was consistent with the results of *in vitro* dissolution experiment (as shown in Fig. 9).

Powder X-Ray Diffraction

In Fig. 12A, there were many diffraction peaks in the PXRD pattern of Mag, indicating that the Mag raw material powder mainly existed in the crystalline state. In the physical mixture, the diffraction peaks decreased obviously. In the diffraction pattern of Mag-NS-SD, the diffraction peaks of Mag basically disappeared, indicating that most of the Mag in Mag-NS-SD changed from crystalline to molecular or amorphous.

Infrared Absorption Spectrum

According to Fig. 12B, the characteristic frequency of -OH in Mag was 3157.6 cm^{-1} . The PM spectrum was similar to the combination of Mag and Blank-NSSD, and the characteristic frequency of -OH was almost invisible in 3157.6 cm^{-1} . In the IR of Mag-NS-SD, the characteristic peak of -OH disappeared completely. The above results indicated that there may be hydrogen bonding between the drug and the carriers in the NS-SD in this study.

Fig. 12 PXRD diagrams (A) and IR spectra (B) of Mag, the physical mixture of Mag and NS-SD (Mag-NS-SD-PM), and the Mag novel supersaturation solid dispersion (Mag-NS-SD)

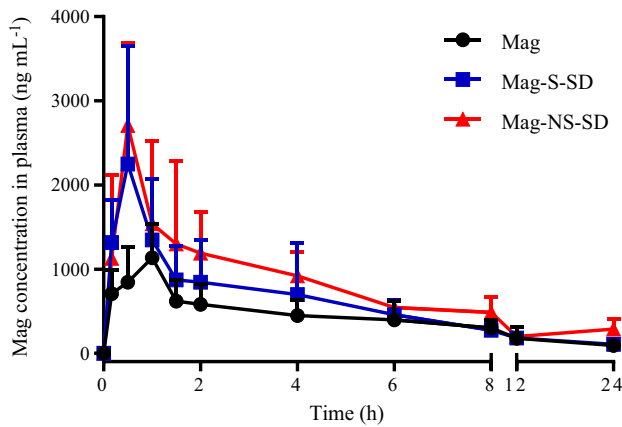
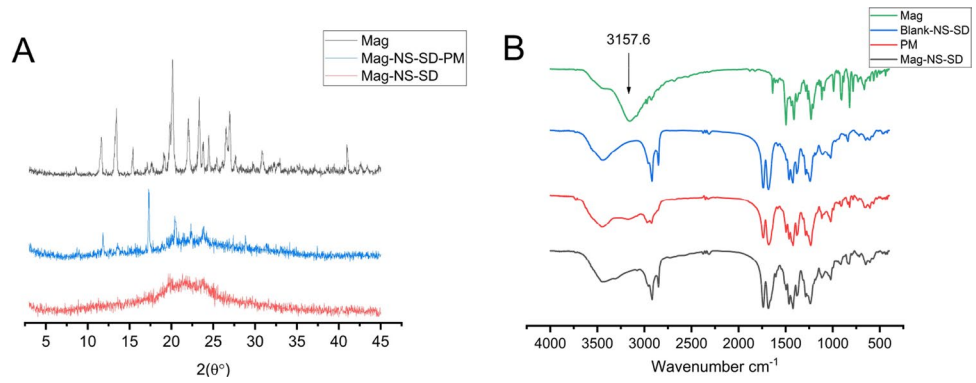


Fig. 13 Mean Mag plasma concentration time curves of the Mag, Mag-S-SD, and Mag-NS-SD in rats ($n = 5$)

In Vivo Pharmacokinetic Study

From Fig. 13 and Table IX, it was known that the absorption of Mag was poor after oral administration, but the oral absorption of Mag was significantly improved after being prepared into Mag-S-SD. Among them, there was no statistical difference in T_{max} and $T_{1/2}$, but there was significant difference of AUC between the groups.

Mag-S-SD compared with Mag, $Fr = 145.12\%$. The reason was that after the solubility of Mag in Mag-S-SD was improved, thus the oral bioavailability of the drug was increased. Still, we realized that this number was limited. The reason was that the dissolution profile of Mag-S-SD was poor (as shown in Fig. 9). And it has a high supersaturation degree, which may result in unsatisfactory drug absorption due to precipitation before drug absorption. Mag-NS-SD could significantly improve AUC_{0-t} compared with Mag or Mag-S-SD. The relative oral bioavailability can reach 213.69% and 142.37% compared with Mag and Mag-S-SD,

Table IX Pharmacokinetic Parameters of Mag, Mag-S-SD, and Mag-NS-SD After Single Dose

	C_{max} ($\mu\text{g}\cdot\text{mL}^{-1}$)	T_{max} (h)	$T_{1/2}$ (h)	AUC_{0-t} ($\mu\text{g}\cdot\text{h}^{-1}\cdot\text{mL}^{-1}$)	F_r (%)
Mag	1.15±0.41	0.9±0.25	9.21±0.31	5.94±1.69	Reference
Mag-S-SD	2.36±1.32	0.53±0.34	9.26±0.38	8.62±1.86	145.12
Mag-NS-SD	2.71±0.99	0.5±0.00	9.97±0.69	12.69±3.07	213.69

$F_r = AUC_{0 \rightarrow T} / AUC_{0 \rightarrow T} \times 100\%$

Fr : relative bioavailability (%)

T : test preparation

R : reference preparation

**Extremely significantly ($P < 0.01$), *significant ($P < 0.05$)

and the oral absorption was obviously improved. The reasons were as follows: *in vitro* experiments showed that Mag-NS-SD significantly increased the supersaturation of Mag (as shown by Table VIII), promoted drug release, and effectively increased the dissolution rate and cumulative release of drugs (as shown by Fig. 9). Although the C_{\max} and T_{\max} of Mag-NS-SD were not significantly improved compared with Mag-S-SD, the two one-side *t*-test showed that Mag-NS-SD was not equivalent to Mag-S-SD (56–58). In addition, AUC_{0-t} of Mag-NS-SD was significantly improved compared with Mag-S-SD, and the bioavailability of Mag-NS-SD was further improved compared with Mag-S-SD.

CONCLUSION

In the present work, Mag-S-SD and Mag-NS-SD were prepared, and the oral bioavailability of Mag *in vivo* was improved by increasing the dissolution profile of Mag. The optimal carrier was screened as PS-630 by composite indicators. The ratio of Mag and PS-630 was determined to be 1:3 by *in vitro* release experiment and particle size determination. On this basis, Mag-NS-SD was prepared by adding self-emulsifying excipients to enhance the drug release rate and oral bioavailability. In this study, the composite center design method was used to determine the optimal conditions for Mag-NS-SD. The release speed was the fastest under the following optimized conditions: Mag:PS-630:MG:LHP = 1:3:0.8:0.266 in mass ratio. The *in vitro* release experiment manifested that the Mag-NS-SD could significantly improve the dissolution of Mag, and the supersaturation degree was significantly increased. Furthermore, the XRD patterns of Mag-S-SD and Mag-NS-SD provided evidence that all APIs were amorphous. The IR spectra of Mag-S-SD and Mag-NS-SD suggested the existence of hydrogen bonding in the systems. In the rat pharmacokinetic study, compared with Mag and Mag-S-SD, the relative oral bioavailability of Mag-NS-SD reached 213.69% and 142.37%, and oral absorption was significantly improved. In short, Mag-NS-SD prepared in this study had the characteristics of rapid release and high oral bioavailability.

Acknowledgements We are grateful that this work was supported by grants from 2020 Liaoning Provincial Department of Education Scientific Research Funding Project—Key Research Project (NO. 2020LZD02) and Open Fund of the State Key Laboratory of New Technology of Chinese Medicine Pharmaceutical Process (No. SKL2020Z0206).

Author Contribution Jing Zhao: conceptualization, methodology, formal analysis, investigation, resources, data curation, writing—review and editing, visualization, supervision, project administration; Pan Gao: conceptualization, methodology, formal analysis, investigation, resources, data curation, writing—original draft, visualization, supervision, project administration; Chengqiao Mu: conceptualization, formal

analysis, investigation, data curation; Jingqi Ning: conceptualization, methodology, data acquisition, formal analysis; Wenbin Deng: conceptualization, methodology, formal analysis, data curation; Dongxu Ji: literature review, writing—original draft, data curation; Haowei Sun: writing—original draft, visualization, supervision; Xiangrong Zhang: conceptualization, methodology, formal analysis, writing—review and editing, project administration; Xinggong Yang: conceptualization, methodology, formal analysis, writing—review and editing, project administration, funding acquisition.

Declarations

Conflict of Interest The authors declare no competing interests.

References

1. Lee BH, Choi SH, Kim HJ, Park SD, Rhim H, Kim HC, *et al.* Gintonin absorption in intestinal model systems. *J Ginseng Res.* 2018;42(1):35–41.
2. Wenlock MC, Austin RP, Barton P, Davis AM, Leeson PD. A comparison of physicochemical property profiles of development and marketed oral drugs. *J Med Chem.* 2003;46(7):1250–6.
3. Mu H, Holm R, Mullertz A. Lipid-based formulations for oral administration of poorly water-soluble drugs. *Int J Pharm.* 2013;453(1):215–24.
4. Dhillon B, Goyal NK, Malviya R, Sharma PK. Poorly water soluble drugs: change in solubility for improved dissolution characteristics a review. *Glob J Pharmacol.* 2014;8(1):26–35.
5. Park H, Ha ES, Kim MS. Current status of supersaturable self-emulsifying drug delivery systems. *Pharmaceutics.* 2020;12(4):365.
6. Higuchi T. Physical chemical analysis of percutaneous absorption process from creams and ointments. *J Soc Cosmet Chem.* 1960;11:85–97.
7. Brouwers J, Brewster ME, Augustijns P. Supersaturating drug delivery systems: the answer to solubility-limited oral bioavailability? *J Pharm Sci.* 2009;98(8):2549–72.
8. Guzman H, Tawa M, Zhang Z, Ratanabanangkoon P, Remenar J. Spring and parachute approach to designing solid celecoxib formulations having enhanced oral absorption. *AAPS J.* 2004;6:21–9.
9. Xu S, Dai WG. Drug precipitation inhibitors in supersaturable formulations. *Int J Pharm.* 2013;453(1):36–43.
10. Gao P, Rush BD, Pfund WP. Development of a supersaturable SEDDS (S-SEDDS) formulation of paclitaxel with improved oral bioavailability. *J Pharm Sci.* 2003;92(12):2386–98.
11. Huang Y, Dai WG. Fundamental aspects of solid dispersion technology for poorly soluble drugs. *Acta Pharm Sin B.* 2013;4(1):18–25.
12. Urbanetz NA, Lippold BC. Solid dispersions of nimodipine and polyethylene glycol 2000: dissolution properties and physico-chemical characterisation. *Eur J Pharm Biopharm.* 2005;59(1):107–18.
13. Tsunashima D, Yamashita K, Ogawara KI, Sako K, Higaki K. Preparation of extended release solid dispersion formulations of tacrolimus using ethylcellulose and hydroxypropylmethylcellulose by solvent evaporation method. *J Pharm Pharmacol.* 2016;68(3):316–23.
14. Pinto JMO, Leão AF, Riekes MK, França MT, Stulzer HK. HPM-CAS as an effective precipitation inhibitor in amorphous solid dispersions of the poorly soluble drug candesartan cilexetil. *Carbohydr Polym.* 2017;2017:199–206.
15. Zhu C, Gong S, Ding J, Yu M, Ahmad E, Feng Y, *et al.* Supersaturated polymeric micelles for oral silybin delivery: the

- role of the Soluplus–PVPVA complex. *Acta Pharm Sin B*. 2019;9(01):107–17.
16. Xia D, Yu H, Tao J, Zeng J, Zhu Q, Zhu C, *et al*. Supersaturated polymeric micelles for oral cyclosporine A delivery: the role of Soluplus–sodium dodecyl sulfate complex. *Colloids Surf B Biointerfaces*. 2016;141:301–10.
 17. Suzuki H, Sunada H. Some factors influencing the dissolution of solid dispersions with nicotinamide and hydroxypropylmethylcellulose as combined carriers. *Chem Pharm Bull*. 1998;46(6):1015–20.
 18. Yongfei L. Preparation and dissolution of resveratrol S-SMEDDS. *Technol Wind*. 2019;36(36):135–7.
 19. Pouton CW. Lipid formulations for oral administration of drugs: non-emulsifying, self-emulsifying and ‘self-microemulsifying’ drug delivery systems. *Euro J Pharm Sci*. 2000;11:93–8.
 20. Guilan Q, Boyi N, Vikramjeet S, Yixian Z, Chuan-Yu W, Xin P, *et al*. Supersaturable solid self-microemulsifying drug delivery system: precipitation inhibition and bioavailability enhancement. *Int J Nanomed*. 2017;12:8801–11.
 21. Li P, Hynes SR, Haefele TF, Pudipeddi M, Royce AE, Serajuddin ATM. Development of clinical dosage forms for a poorly water-soluble drug II: formulation and characterization of a novel solid microemulsion preconcentrate system for oral delivery of a poorly water-soluble drug. *J Pharm Sci*. 2010;98(5):1750–64.
 22. Chavan RB, Modi SR, Bansal AK. Role of solid carriers in pharmaceutical performance of solid supersaturable SEDDS of celecoxib. *Int J Pharm*. 2015;495(1):374–84.
 23. Agarwal V, Siddiqui A, Ali H, Nazzal S. Dissolution and powder flow characterization of solid self-emulsified drug delivery system (SEDDS). *Int J Pharm*. 2008;366(1–2):44–52.
 24. Lin MH, Chen MC, Chen TH, Chang HY, Chou TC. Magnolol ameliorates lipopolysaccharide-induced acute lung injury in rats through PPAR- γ -dependent inhibition of NF- κ B activation. *Int Immunopharmacol*. 2015;28(1):270–8.
 25. Lin CF, Hwang TL, Al-Suwayeh SA, Huang YL, Fang JY. Maximizing dermal targeting and minimizing transdermal penetration by magnolol/honokiol methoxylation. *Int J Pharmaceut*. 2013;445(1):153–62.
 26. Pacult J, Rams-Baron M, Chrzaszcz B, *et al*. Effect of polymer chain length on the physical stability of amorphous drug-polymer blends at ambient pressure. *Mol Pharm*. 2018;15(7):2807–15.
 27. Li Y, Lu M, Wu C. PVP VA64 as a novel release-modifier for sustained-release mini-matrices prepared via hot melt extrusion. *Drug Deliv Transl Res*. 2018;8(6):1670–8.
 28. Xia D, Yu H, Tao J, Zeng J, Zhu Q, Zhu C, *et al*. Supersaturated polymeric micelles for oral cyclosporine A delivery: the role of Soluplus-sodium dodecyl sulfate complex. *Colloids Surf B*. 2016;141:301–10.
 29. Yu H, Xia D, Zhu Q, Zhu C, Chen D, Gan Y. Supersaturated polymeric micelles for oral cyclosporine A delivery. *Eur J Pharm Biopharm*. 2013;85(3):1325–36.
 30. Hancock BC, York P, Rowe RC. The use of solubility parameters in pharmaceutical dosage form design. *Int J Pharm*. 1997;148(1):1–21.
 31. Kuentz M, Holm R, Elder DP. Methodology of oral formulation selection in the pharmaceutical industry. *Eur J Pharm Sci*. 2016;87:136–63.
 32. Forster A, Hempenstall J, Tucker I, Rades T. Selection of excipients for melt extrusion with two poorly water-soluble drugs by solubility parameter calculation and thermal analysis. *Int J Pharm*. 2001;226(1–2):147–61.
 33. Li PLX, Zhou H. Prediction method for the compatibility between drug and carrier. *Chin J New Drugs*. 2009;18(3):262–71.
 34. Zhang HSL, Wang Y. Research progress on excipients of solid dispersion prepared by hot-melt extrusion technique. *Drug Clinic*. 2014;29(5):557–63.
 35. Lu Y, Xu Z. Optimization of curcumin solid dispersion formulation and *in vitro* dissolution evaluation. *Herb Depot*. 2021;30(2):31–7.
 36. Fedors RF. A method for estimating both the solubility parameters and molar volumes of liquids. *Polym Eng Sci*. 1974;14(2):147–54.
 37. El-Banna HM, Daabis NA, Mortada LM, Abd-Elfattah S. Physicochemical study of drug binary systems. Part 3: tolbutamide-urea and tolbutamide-mannitol systems. *Pharmazie*. 1976;30(12):788–92.
 38. Nakai Y, Yamamoto K, Oguchi T, *et al*. Determination of solubility parameters for solid medicinals and excipients. *J Pharmacobiodyn*. 1989;12(2):20–3.
 39. Rhodes CT. Drug development and industrial pharmacy. *Drug Dev Commun*. 1995;21(20):2263–85.
 40. Bloch DW, Elegakey MA, Speiser PP. Solid dispersion of chlorthalidone in urea phase diagram and dissolution characteristics. *Pharm Acta Helv*. 1982;57(8):231–5.
 41. Li J, Jiang ZT. Preparation and bioavailability of magnolol solid dispersions. *Chin Trad Herb Drugs*. 2019;14(50):3337–44.
 42. Bavishi DD, Borkhataria CH. Spring and parachute: how cocrystals enhance solubility. *Prog Cryst Growth Charact Mater*. 2016;62(3):1–8.
 43. Zhu C, Gong S, Ding J, Yu M, Ahmad E, Feng Y, *et al*. Supersaturated polymeric micelles for oral silybin delivery: the role of the Soluplus-PVPVA complex. *Acta Pharm Sin B*. 2019;9(1):107–17.
 44. Yamashita T, Ozaki S, Kushida I. Solvent shift method for anti-precipitant screening of poorly soluble drugs using biorelevant medium and dimethyl sulfoxide. *Int J Pharm*. 2011;419(1):170–4.
 45. Ahn J-H, Kim Y-P, Lee Y-M, Seo E-M, Lee K-W, Kim H-S. Optimization of microencapsulation of seed oil by response surface methodology. *Food Chem*. 2008;107(1):98–105.
 46. Das SS, Singh A, Kar S, Ghosh R, Pal M, Fatima M, *et al*. Application of QbD framework for development of self-emulsifying drug delivery systems. In: *Pharmaceutical Quality by Design*. 2019. p. 297–350.
 47. Dian L, Yu E, Chen X, Wen X, Zhang Z, Qin L, *et al*. Enhancing oral bioavailability of quercetin using novel soluplus polymeric micelles. *Nanoscale Res Lett*. 2014;9(1):2406.
 48. Wang L, Huang T, Zeng J. Application progress of copolymer Soluplus® in new pharmaceutical formulations and technologies. *Chin Pharm*. 2016;27(19):2703–7.
 49. Jiang WLY. Progress of applications of copovidone to pharmaceutical preparations. *Chin J Pharm*. 2015;46(8):898–903.
 50. Ma F, Li X, Yin J, Ma L, Li D. Optimisation of double-enzymatic extraction of arabinoxylan from fresh corn fibre. *J Food Sci Technol*. 2020;57:1–11.
 51. Dilpreet S, Manisha S, K TA, Neena B. Evaluation of biomechanistic behavior of liquid self-microemulsifying drug delivery system in biorelevant media. *Assay Drug Dev Technol*. 2020;19:85–96.
 52. Ujhelyi Z, Vecsernyés M, Fehér P, Kósa D, Arany P, Nemes D, *et al*. Physico-chemical characterization of self-emulsifying drug delivery systems. *Drug Discov Today Technol*. 2018;27:81–6.
 53. Zhong L, Li X, Liu L, Liao Y, Tang H, Xie L, *et al*. Research progress on application and curing of self-microemulsion in traditional Chinese medicine preparation. *Pharm Clinic Chin Mater Med*. 2019;10(2):53-8+64.

54. Gong L, Liao G, Chen Q, Luan H, Feng Y. Swollen surfactant micelles: properties and applications. *Acta Phys Chim Sin.* 2019;35(8):816–28.
55. Chen P. Molecular interfacial phenomena of polymers and biopolymers. *Mater Today.* 2005;8(11):62–3.
56. Ding T. Application of EXCEL in statistical test of bioequivalence. *Chin Pharm.* 2007;2007(01):93–4.
57. Han W, Jiang J. Overview of statistical evaluation methods for bioequivalence. *Chin J Health Stat.* 2010;27(04):441–5.
58. Sun W, Sun R. Two one side t-test for computational simplicity of bioavailability equivalence. *Chin J Clin Pharmacol Ther.* 1997;04:279–82.

Publisher's Note Springer Nature remains neutral with regard to jurisdictional claims in published maps and institutional affiliations.